JOC Article

Through-Shell Alkyllithium Additions and Borane Reductions

Ralf Warmuth,*[,†,‡] Emily F. Maverick[‡], Carolyn B. Knobler[‡], and Donald J. Cram[‡,§]

Department of Chemistry, Kansas State University, Manhattan, Kansas 66506-3701, and Department of Chemistry and Biochemistry, University of California at Los Angeles, Los Angeles, California 90095-1569

warmuth@ksu.edu

Received November 3, 2002

The through-shell borane reduction and methyllithium addition to benzaldehyde (**1**), benzocyclobutenone (**2**), and benzocyclobutenedione (**3**) incarcerated inside a hemicarcerand (**4**) with four tetramethylenedioxy bridges are reported. All guests could be reduced and methylated. Selective monoreduction and monomethylation were observed for **3**. In the methyllithium addition to **4**⊙**3**, the initially formed lithium alcoholate underwent a Moore rearrangement. The reactivity of the incarcerated guests toward methyllithium increased in the order **1** < **2** ≪ **3** and toward borane in the order **1** ≪ **2** ≈ **3**. Guest reactivity was correlated with the inner-phase location of the reacting carbonyl group in the preferred guest inner-phase orientation. The latter was determined from the X-ray structures of **4**⊙**1**, **4**⊙**2**, and **4**⊙**3**, from molecular mechanical calculations, and from the hemicarcerand-induced upfield shift of the guest proton resonances. In the methyllithium and *n*-butyllithium addition to **4**⊙**1** and **4**⊙**3** at elevated temperatures, selective cleavage of a host's spanner or tetramethylenedioxy bridge, respectively, was observed. The cleavage of one spanner also took place in the methyllithium addition to the 1-methyl-2-pyrrolidinone hemicarceplex. These scission reactions are initiated by the initially formed lithium alcoholates, which show enhanced basicity and nucleophilicity in the inner phase as compared to the bulk phase. Mechanisms for the host scission reactions are discussed.

Introduction

Carcerands and hemicarcerands are spherical hosts with a well-defined, enforced inner cavity—the inner phase—which provides enough space for the incarceration of one or more guest molecules.[1,2] The guest is held within the host by constrictive binding energy, which is a new binding phenomenon.[3] Constrictive binding energy is the activation energy required for a guest to enter the inner cavity of a hemicarcerand through one of the size-restricted equatorial portals. In many hemicarcerands, these equatorial portals are large enough to allow bulk-phase reactants to enter and exit the inner phases and to undergo inner-phase reactions with the incarcerated guest.[4−14] Some of these reactions are truly inner-phase reactions, in which all reactants are fully incarcerated, whereas others probably take place in one of the equatorial entryways. The latter are better described as through-shell reactions and are particularly interesting since the size, shape, and polarity of the host's portals is expected to have a strong influence on the stability of such through-shell transition states. The concepts of *inner-phase chemistry* and *through-shell reactions* give rise to many interesting questions. For example, how would an inner-phase reaction differ from its counterpart carried

† Kansas State University.

‡ University of California at Los Angeles.

§ Deceased June 17, 2001.

(1) (a) Cram, D. J.; Karbach, S.; Kim, Y. H.; Baczynskyj, L.; Kalleymeyn, G. W. *J. Am. Chem. Soc.* **1985**, *107*, 2575−6. (b) Cram, D. J. *Nature* **1992**, *356*, 29−36. (c) Cram, D. J.; Cram, J. M. In *Container Molecules and Their Guests*; Monographs in Supramolecular Chemistry, No. 4; Stoddart, J. F., Series Ed.; The Royal Society of Chemistry: Cambridge, U.K., 1994. (d) Jasat, A.; Sherman, J. C. *Chem. Rev.* **1999**, *99*, 931−967. (e) Warmuth, R.; Yoon, J. *Acc. Chem. Res.* **2001**, *34*, 95−105.

(2) (a) Mungaroo, R.; Sherman, J. C. *Chem. Commun.* **2002**, 1672−1673. (b) Chopra, N.; Sherman, J. C. *Angew. Chem., Int. Ed.* **1999**, *38*, 1955−1957. (c) Naumann, C.; Place, S.; Sherman, J. C. *J. Am. Chem. Soc.* **2002**, *124*, 16−17.

(3) Cram, D. J. *Angew. Chem., Int. Ed. Engl.* **1988**, *27*, 1009−1020.

(4) Warmuth, R. *J. Inclusion Phenom.* **2000**, *37*, 1−38.

(5) Robbins, T. A.; Cram, D. J. *J. Am. Chem. Soc.* **1993**, *115*, 12199−12200.

(6) Cram, D. J.; Tanner, M. E.; Thomas, R. *Angew. Chem.* **1991**, *103*, 1048−1051; *Angew. Chem., Int. Ed. Engl.* **1991**, *30*, 1024−1027.

(7) Warmuth, R.; Marvel, M. A. *Chem.—Eur. J.* **2001**, *7*, 1209−1220.

(8) Warmuth, R. *Angew. Chem.* **1997**, *109*, 1406−9; *Angew. Chem. Int. Ed. Engl.* **1997**, *37*, 1347−1350.

(9) Kurdistani, S. K.; Helgeson R.; Cram, D. J. *J. Am. Chem. Soc.* **1995**, *117*, 1659−1660.

(10) Cram, D. J.; Tanner, M. E.; Knobler, C. B. *J. Am. Chem. Soc.* **1991**, *113*, 7717−7726.

(11) (a) Farran, A.; Deshayes, K. D.; Matthews, C.; Balanescu, I. *J. Am. Chem. Soc.* **1995**, *117*, 9614−9615. (b) Farran, A.; Deshayes, K. D. *J. Phys. Chem.* **1996**, *100*, 3305−3307. (c) Pina, F.; Parola, A. J.; Ferreira, E.; Maestri, M.; Armaroli, N.; Ballardini, R.; Balzani, V. *J. Phys. Chem.* **1995**, *99*, 12701−12703. (d) Parola, A. J.; Pina, F.; Ferreira, E.; Maestri, M.; Balzani, V. *J. Am. Chem. Soc.* **1996**, *118*, 11610−11616. (e) Place, I.; Farrán, A.; Deshayes, K.; Piotrowiak, P. *J. Am. Chem. Soc.* **1998**, *120*, 12626−12633. (f) Romanova, Z. S.; Deshayes, K.; Piotrowiak, P. *J. Am. Chem. Soc.* **2001**, *123*, 11029−11036. (g) Mendoza, S.; Davidov, P. D.; Kaifer, A. E. *Chem.—Eur. J.* **1998**, *4*, 864−870.

(12) Yoon, J.; Nakamura, K. *Bull. Korean Chem. Soc.* **1999**, *20*, 765−767.

(13) Cram, D. J.; Blanda, M. T.; Paek, K.; Knobler, C. B. *J. Am. Chem. Soc.* **1992**, *114*, 7765−7773.

(14) (a) Kang, J.; Rebek, J. Jr. *Nature* **1996**, *385*, 50−52. (b) Kang, J.; Santamaría, J.; Hilmersson, G.; Rebek, J., Jr. *J. Am. Chem. Soc.* **1998**, *120*, 7389−7390. (c) Kang, J.; Hilmersson, G.; Santamaría, J.; Rebek, J., Jr. *J. Am. Chem. Soc.* **1998**, *120*, 3650−3656.

10.1021/jo026649z CCC: $25.00
Published on Web 02/14/2003

CHART 1

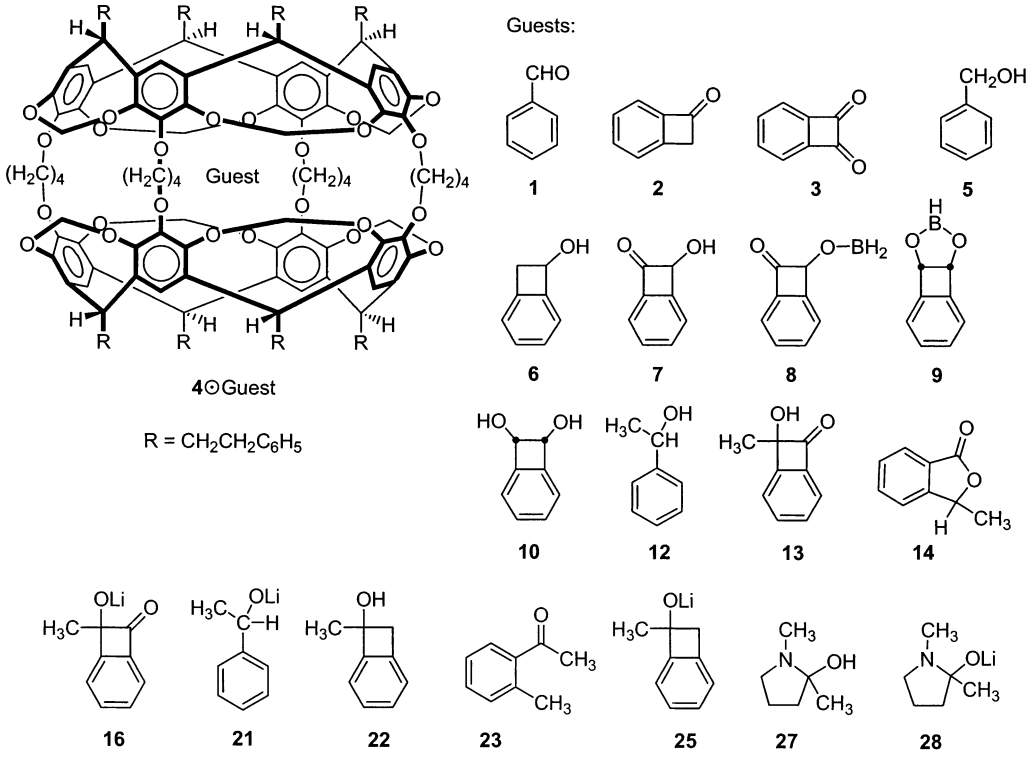

out in bulk phases? Could one completely reverse the course of a reaction by disfavoring low-energy solution pathways and favoring high-energy pathways through incarceration? Would it be possible to change the regio- and stereoselectivity of reactions?[9] How would the surrounding host alter the reactivity of the incarcerated guest?[15−18]

A main objective of our research efforts is to explore the scope of inner-phase reactions and through-shell reactions and to investigate the effect of cavity constraint, portal size, and portal shape on guest reactivity. Such research can lead to the development of artificial enzymes: tailored hemicarcerands as unimolecular reaction flasks that mimic the binding sites of enzymes and allow one to perform highly stereo- and regioselective transformations of molecules incarcerated in their inner phases.

Here we report a detailed investigation of through-shell reactions involving bulk-phase organometallic reactants and also the highly selective borane reduction of benzaldehyde (**1**), benzocyclobutenone (**2**), and benzocyclobutenedione (**3**) inside the known hemicarcerand **4**.[19] We have chosen guests **1**−**3** for two reasons: (1) The three guests have different shapes, leading to different orientations of their carbonyl groups with respect to the equatorially located portals of hemicarcerand **4**. (2) The three guests have carbonyl groups with different reactivities, which increase in bulk-phase reactions in the order **3** ≈ **2** < **1**. Our investigation shows that the order of reactivity is strongly altered by incarceration. Furthermore, in the course of our investigations, we discovered several interesting reactions between the intermediary, incarcerated lithium alcoholates and the surrounding hemicarcerand leading to the controlled scission of the host and an enlargement of one of its portals. In particular, we report the first hemicarcerand with a missing spanner group. Previous work has shown that such hemicarcerands with one extended portal are very useful for the incarceration of large and/or thermally sensitive guests.[7,9,20]

Results and Discussion

See Chart 1 for the structures of most of the compounds discussed in this paper.

Synthesis of Hemicarceplexes. We prepared the 1-methyl-2-pyrrolidinone (NMP) hemicarceplex **4**⊙NMP as described for the corresponding *N*,*N*-dimethylacetamide (DMA) hemicarceplex **4**⊙DMA by replacing the solvent DMA by NMP.[19,20] Refluxing **4**⊙NMP in diphenyl ether for 2 days gave hemicarcerand **4**.[19] We prepared hemicarceplex **4**⊙**3** as described earlier.[8] Heating empty **4** in neat **1** or **2** at 150−170 °C yields **4**⊙**1** (95% yield) and **4**⊙**2** (80% yield), respectively.

Through-Shell Borane Additions. In CPK models, diborane is small enough to pass through one of the host's equatorial portals and hence is suitable for inner-phase reductions. Indeed, refluxing **4**⊙**1** for 16 h in a BH_3·THF

(15) Warmuth, R. *J. Chem. Soc., Chem. Commun.* **1998**, 59−60.
(16) Körner, S. K.; Tucci, F. C.; Rudkevich, D. M.; Heinz, T.; Rebek, J., Jr. *Chem.—Eur. J.* **2000**, *6*, 188−195.
(17) Warmuth, R.; Kerdelhué, J.-L.; Sánchez Carrera, S.; Langenwalter, K. J.; Brown, N. *Angew. Chem., Int. Ed.* **2002**, *41*, 96−99.
(18) van Wageningen, A. M. A.; Timmerman, P.; van Duynhoven, J. P. M.; Verboom, W.; van Veggel, F. C. J. M.; Reinhoudt, D. N. *Chem.—Eur. J.* **1997**, *3*, 639.
(19) Robbins, T.; Knobler, C. B.; Bellew, D.; Cram, D. J. *J. Am. Chem. Soc.* **1994**, *116*, 111−122.
(20) Yoon, J.; Sheu, C.; Houk, K. N.; Knobler, C. B.; Cram, D. J. *J. Org. Chem.* **1996**, *61*, 9323−9339.

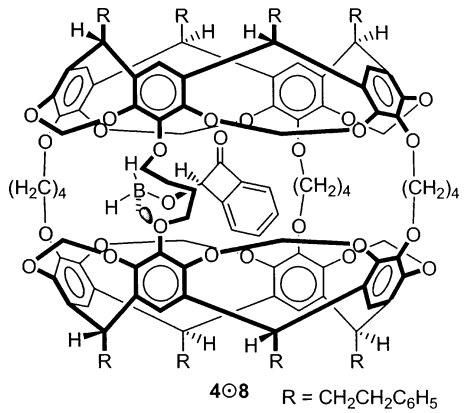

FIGURE 1. Proposed guest orientation of **8** inside the inner phase of hemicarcerand **4**.

in THF solution (1 M) did give incarcerated benzyl alcohol **4**⊙**5**, but in only 13% yield, together with 65% unreacted **4**⊙**1** and 15% tetrahydrofuran hemicarceplex **4**⊙THF.[11] The latter hemicarceplex results most likely from dissociation of **4**⊙**1** and/or **4**⊙**5** followed by incarceration of a solvent molecule into empty **4** during the reaction. Comparison with an authentic sample prepared by heating empty **4** in benzyl alcohol (170 °C, 70 h, 95% yield) confirmed the formation of **4**⊙**5**. In contrast to their bulk-phase reactivity, the through-shell reduction of incarcerated **2** and **3** is faster than the reduction of incarcerated **1**. Refluxing **4**⊙**2** or **4**⊙**3** in excess BH_3·THF in THF (1 M) (**4**⊙**2**, 40 h; **4**⊙**3**, 49 h) gave 85% **4**⊙**6** and 5% **4**⊙THF for the reduction of **4**⊙**2** (90% conversion), and 86−90% **4**⊙**7** and ca. 5% **4**⊙THF for the reduction of **4**⊙**3** (91−95% conversion). The tetrahydrofuran hemicarceplex most likely was formed via a dissociation/complexation sequence analogous to that described above. Interestingly, despite the large excess of the reducing agent, the through-shell reduction of **4**⊙**3** led to selective monoreduction in contrast to bulk-phase reductions of α-diketones.

The preferred monoreduction must be a consequence of the inaccessibility of the carbonyl group of **8** to the bulk-phase BH_3·THF complex. We assume a guest orientation inside the inner phase such that the borane is located close to an equatorial host portal and the carbonyl is in the inner space of a host's cavitand (Figure 1). In this orientation, Lewis complex formation between the borane and an inward-pointing oxygen electron lone pair of a tetramethylenedioxy bridge or a solvent molecule is possible. The energetic burden associated with guest reorientation in addition to steric factors might prevent the through-shell interaction of the second carbonyl oxygen with a bulk-phase borane molecule, which is required for further reduction.

However, after aqueous workup and chromatographic purification of **4**⊙**7**, refluxing **4**⊙**7** in excess 1 M BH_3·THF in THF for 90 h reduced guest **7** to the dioxyborolane **9** in 85% yield. The shell of **4** protects the guest, which survived the aqueous workup. Hydrolysis in water-saturated $CHCl_3$ at room temperature afforded the corresponding *cis*-benzocyclobutene-7,8-diol hemicarceplex **4**⊙**10** and required several weeks. The insensitivity of **9** toward hydrolysis can be rationalized by its inner-phase orientation, suggested by the hemicarcerand-induced upfield shift $\Delta\delta$ of the guest protons. The ^{1}H NMR spectrum of hemicarceplex **4**⊙**9** is shown in Figure 2. From $\Delta\delta$(H1) 0.91 and $\Delta\delta$(H2) 3.43 of the guest protons,[21,22] we predict that the favored orientation of the elliptical guest is such that the borolane hydrogen is located in the shielded region of one of the two cavitands of **4**, which explains the low reactivity of **9**. The broadening of the signal assigned to the eight inward-pointing H_i atoms of the methylene spanners of **4** (δ 4−4.7) is most likely due to the restricted rotation of **9** around the equatorial C_2 axis of **4** and is consistent with the shape, the predicted orientation, and the reactivity of **9** in the inner phase.

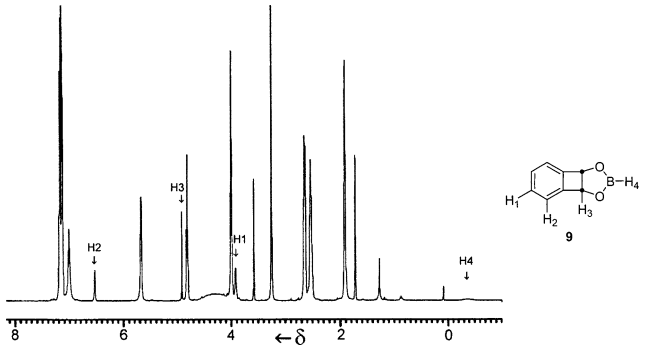

FIGURE 2. ^{1}H NMR spectrum (500 MHz in $(CD_2)_4O$ at 25 °C) of hemicarceplex **4**⊙**9**. Signals assigned to the guest protons are marked with arrows.

^{11}B NMR studies confirmed the formation of **9**. Due to quadrupole broadening, the ^{1}H-coupled ^{11}B NMR spectrum of **4**⊙**9** shows a broad ^{11}B signal (line width 12.6 ppm) at δ 28.3 relative to that of BF_3·$O(C_2H_5)_2$ (δ 0) with no fine structure. The measured chemical shift is consistent with the postulated structure of **9**; e.g., δ 28.1 for 1,3,2-dioxaborolane (**11**).[23]

11

Room-Temperature Methyllithium Addition to Incarcerated Benzaldehyde. Addition of excess methyllithium (MeLi) to **4**⊙**1** below 0 °C resulted in no reaction. After 9 h at room temperature, 11% expected product **4**⊙**12** was formed and was isolated together with 65% unreacted hemicarceplex **4**⊙**1**. The addition of *N*,*N*,*N*′,*N*′-tetramethylethylenediamine (TMEDA) to this reaction mixture did not alter the outcome, suggesting that the low reactivity of the incarcerated guest is not a result of a higher aggregation state of MeLi. Comparison of the product ^{1}H NMR with that of an authentic sample prepared by heating empty **4** in 1-phenylethanol (170 °C, 70 h, 95% yield) confirms the formation of **4**⊙**12**.

(21) We used the proton chemical shifts of free *cis*-benzocyclobutene-7,8-diol (**10**) in $CDCl_3$ to estimate those of free **9**. *cis*-Benzocyclobutene-7,8-diol was prepared via $NaBH_4$ reduction of **1** and showed spectral data identical to those reported by Boyd et al. (ref 22).

(22) Boyd, D. R.; Sharma, N. D.; Stevenson, P. J.; Chima, J.; Gray, D. J.; Dalto, H. *Tetrahedron Lett.* **1991**, *32*, 3887−3890.

(23) (a) McAchran, G. E.; Shore, S. G. *Inorg. Chem.* **1966**, *5*, 2044−2046. (b) Nöth, H.; Wrackmeyer, B. In *NMR. Basic Principles and Progress*; Diehl, P., Fluck, E., Kosfeld, R., Eds.; Springer-Verlag: New York, 1978; Vol. 14, p 5.

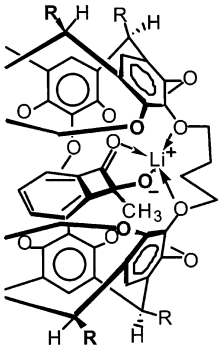

FIGURE 3. Schematic representation of the proposed orientation of lithium alcoholate **16** in the inner phase of hemicarcerand **4**. This orientation provides sufficient coordination of the lithium cation by electron lone pairs of the alcoholate and a tetramethylenedioxy bridge of **4**.

Methyllithium Addition at −78 °C to Incarcerated Benzocyclobutenedione. The addition of excess methyllithium to a solution of **4**⊙**3** in THF/Et_2O at −78 °C followed by H_2O quench at −78 °C after 30 h resulted in the formation of two new hemicarceplexes, **4**⊙**13** (65%) and **4**⊙**14** (25%). Although a large excess of MeLi was used, no double addition product **15** was formed in this through-shell addition reaction.

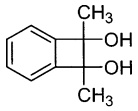

15

We assume that the initially formed lithium alcoholate **16** has an inner-phase orientation which allows the coordination of the lithium cation to the alkoxide and carbonyl oxygen of **16** and to an inward-pointing electron lone pair of each of the two oxygens of a tetramethylenedioxy bridge as shown in Figure 3. In this orientation, the addition of a second equivalent of MeLi will be difficult.

While the product **4**⊙**13** was expected, the formation of **4**⊙**14** is more surprising. Moore showed that α-hydroxycyclobutenones thermally rearrange to furanones.[24,25] An inner-phase Moore rearrangement of 8-hydroxy-8-methylbenzocyclobuten-7-one (**13**) could explain the formation of 7-methylphthalide (**14**). Since hemicarceplex **4**⊙**13** is thermally stable at room temperature, it is unlikely that this rearrangement took place at room temperature during the workup. We explain the formation of **4**⊙**14** as follows (Figure 4). The through-shell MeLi addition leads to lithium alcoholate **16**. Due to the shielding nature of the surrounding hemicarcerand, addition of water at −78 °C does not quench **16** at this temperature. When the temperature is raised, **16** rearranges to **17** via the quinodimethane **18a,b**, similar to the Moore rearrangement mentioned above.[24,25] At a temperature sufficiently high for water to enter the cavity

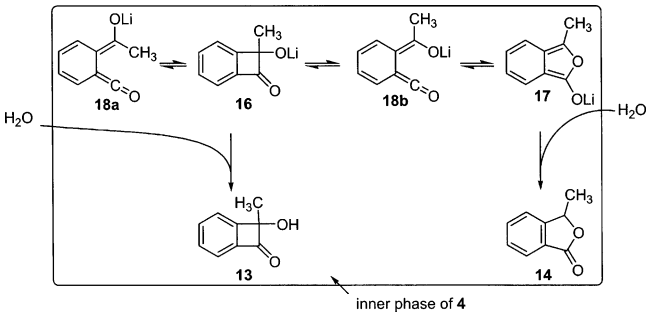

FIGURE 4. Proposed mechanism for the formation of **4**⊙**13** and **4**⊙**14** upon addition of methyllithium to **4**⊙**3**.

of **4**, the inner-phase quench of this equilibrium mixture yields guests **13** and **14** (Figure 4). We conclude that the rearrangement of **16** takes place only upon raising the temperature from −78 °C to room temperature and not earlier, at −78 °C, since (1) **13** but not **14** is isolated upon addition of 1 equiv of MeLi to free benzocyclobutenedione at −78 °C followed by water quench at −78 °C[25] and (2) Swenton et al. previously observed a similar rearrangement for a noncomplexed benzocyclobutenedione/vinyllithium adduct in solution only after warming this adduct to room temperature with the exclusion of water.[26]

Methyllithium Addition at 0 °C to Incarcerated Benzocyclobutenedione. To our surprise, the same reaction, carried out at −10 or 0 °C, gave only trace amounts (<5%) of the previously observed products as determined from the integration of the characteristic upfield-shifted methyl protons of **13** and **14** in the ^{1}H NMR spectrum of the crude reaction mixture. Instead, we isolated diol host **19** (X = H)[9,20] as the main product in 70% yield. We explain the cleavage of both ether C−O bonds of a tetramethylenedioxy bridge of **4** via two subsequent base-induced *β*-eliminations. The following observation supports the action of incarcerated lithium alcoholate **16** or **17** and not bulk-phase methyllithium to initiate the cleavage of the first C−O bond: Methyllithium does not cleave diol host **19** (X = H) or the benzene hemicarceplex **4**⊙C_6H_6[27] under the same conditions (excess MeLi, 0 °C, 8 h, THF/ether). We conclude that the first ether bond cleavage must be initiated via hemicarcerand deprotonation by the incarcerated lithium alcoholate, yielding **20** (X = Li) (Figure 5). Subsequent cleavage of the second ether linkage most likely proceeds via methyllithium, a stronger base than the alcoholate.

Interestingly, alcoholates in general are too weak as bases to induce cleavage of ethers via *β*-elimination. In control experiments, lithium alcoholate **21** (0.4 M) does not cleave the toluene hemicarceplex **4**⊙$C_6H_5CH_3$[28] even after 14 days at 0 °C or after 24 h in refluxing THF/hexane. This corresponds to a rate acceleration for the innermolecular *β*-elimination by a factor of $\gg 10^4$ compared to the intermolecular *β*-elimination. The inner-phase lithium alcoholate concentration is about 8 mol/L,

(24) (a) Perri, S. T.; Foland, L. D..; Decker, O. H. W.; Moore, H. W. *J. Org. Chem.* **1986**, *51*, 3068−3070. (b) Foland, L. D.; Karlsson, J. O.; Perri, S. T.; Schwabe, R.; Xu, S. J.; Patil, S.; Moore, H. W. *J. Am. Chem. Soc.* **1989**, *111*, 975−989.

(25) (a) Liebeskind, L. S.; Iyer, S.; Jewell, C. F., Jr. *J. Org. Chem.* **1986**, *51*, 3067−3068. (b) Liebeskind, L. S. *Tetrahedron* **189**, *45*, 3053−3060.

(26) Swenton, J. S.; Jackson, D. K.; Manning, M. J.; Raynolds, P. W. *J. Am. Chem. Soc.* **1978**, *100*, 6182−6188.

(27) Hemicarceplex **4**⊙C_6H_6 was prepared as described in ref 19 and gave a ^{1}H NMR spectrum that is consistent with the spectrum reported in ref 19.

(28) (a) Kerdelhué, J.-L.; Langenwalter, K. J.; Warmuth, R. *J. Am. Chem. Soc.* **2003**, *125*, 973−986. (b) Makeiff, D. A.; Pope, D. J.; Sherman, J. C. *J. Am. Chem. Soc.* **2000**, *122*, 1337−1342.

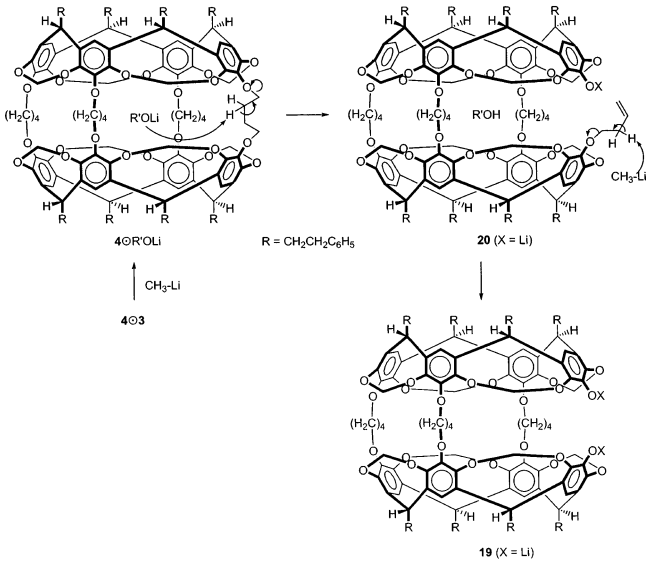

FIGURE 5. Mechanism for base-induced cleavage of **4⊙3** to yield the diol host **19** (X = Li).

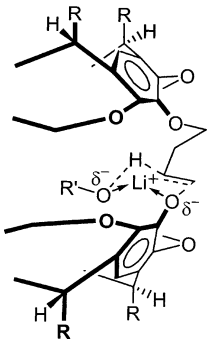

FIGURE 6. Proposed transition state for the lithium alkoxide-induced cleavage of hemicarcerand **4**, yielding hemicarcerand **20** (X = Li).

on the basis of an inner-phase volume of approximately 200 Å^3, which we estimated from the X-ray structures of **4⊙1**, **4⊙2**, and **4⊙3** (see below). Even if we take the 20-fold higher local concentration into account, the inner molecular β-elimination is still more than 100-fold faster than the intermolecular β-elimination. Three factors might contribute to this rate acceleration: (1) the absence of aggregation of the alcoholate in the inner phase,[29] (2) the poor ability of **4** to "solvate" the incarcerated alcoholate, leading to an increased basicity,[10] (3) lithium coordination by the alkoxide lone pair and an oxygen lone pair of the cleaved C−O bond. Coordination fixes the alkoxide oxygen in close proximity to the β-hydrogen of the bridge. Via a six-membered transition state the lithium cation can efficiently compensate for the buildup of negative charge at the phenoxide during the concerted *syn*-elimination (Figure 6).[30]

Butyllithium Addition at −78 °C to Incarcerated Benzocyclobutenedione. Upon addition of *n*-butyllithium (*n*-BuLi) at −78 °C to **4⊙3** in hexane/THF (1:5) in the presence of TMEDA, no products could be isolated corresponding to **13** or **14**; these would, according to CPK models, emerge partially from the inner phase through one equatorial portal. However, small amounts of the diol host **19** (X = H) (10%) and host **20** (X = H) (10%) were isolated together with recovered starting material (62%). Both products are probably formed via the mechanism outlined above. Control experiments show the stability of **4** toward *n*-BuLi under the chosen conditions. This, and in particular the isolation of **20** (X = H), indicates that *n*-BuLi slowly adds to incarcerated **3** and that **19** is formed via the mechanism described above. Steric hindrance due to the larger butyl group probably prevents a faster reaction and hence a higher yield during the reaction time of 12 h. Such a bulk-phase reactant size selectivity was previously observed by Kurdistani et al. in their studies of the alkylation and isotopic exchanges of various incarcerated phenols.[9] Better spatial fixation of the alcoholate in the vicinity of an equatorial portal, due to the butyl substituent, may lead to β-elimination at −78 °C, which is faster than the addition of *n*-BuLi to incarcerated **3**.

Methyllithium Addition to Incarcerated Benzocyclobutenone. A completely different reaction behavior was observed for **4⊙2**. Addition of MeLi to **4⊙2** in THF/ether below −6 °C resulted in no reaction. After 5 h at room temperature a complex product mixture formed, composed of the 7-methylbenzocyclobuten-7-ol hemicarceplex **4⊙22** (25%), the 2-methylacetophenone hemicarceplex **4⊙23** (ca. 1%, as determined from the integration of the characteristic guest signal at δ −1.40 in the ^{1}H NMR spectrum of the crude product mixture), and the hemicarcerand **24** (25%) and its 2-methylacetophenone hemicarceplex **24⊙23** (40%). We supported our assignment by comparison with authentic samples prepared as follows: Formation of **4⊙23** by heating empty **4** in neat 2-methylacetophenone failed. However, heating empty **24**, which has one enlarged portal due to the missing spanner, in neat **23** gave **24⊙23**. The latter can be converted into **4⊙23** with $BrCH_2Cl/K_2CO_3$ in DMF (80% yield).[31] Irradiation of incarcerated **23** at $\lambda > 300$ nm in $CDCl_3$ gave **4⊙22** via photoinduced electrocyclization.[32]

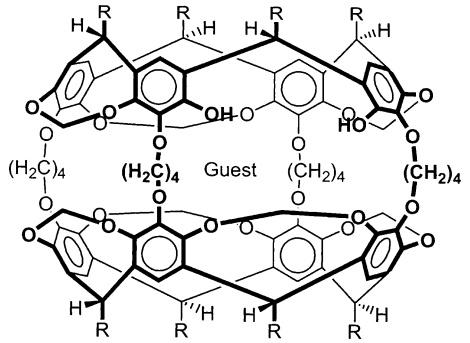

Our proposed mechanism to explain the formation of **24** is related to the S_N2cA mechanism of acetal cleavage

(29) Exner, J. H.; Steiner, E. C. *J. Am. Chem. Soc.* **1974**, *96*, 1782−1787.

(30) (a) Bartsch, R. A. *Acc. Chem. Res.* **1975**, *8*, 239−245. (b) Sicher, J. *Angew. Chem.* **1972**, *84*, 177−191; *Angew. Chem., Int. Ed. Engl.* **1972**, *11*, 200−214.

(31) Using the same strategy, we prepared authentic **4⊙14** via the sequence **24** + **13** → **24⊙14**; **24⊙14** + $BrCH_2Cl$ + K_2CO_3 → **4⊙14** to prove the formation of **4⊙14** in the MeLi addition to **4⊙3** at −78 °C (see also the Experimental Section).

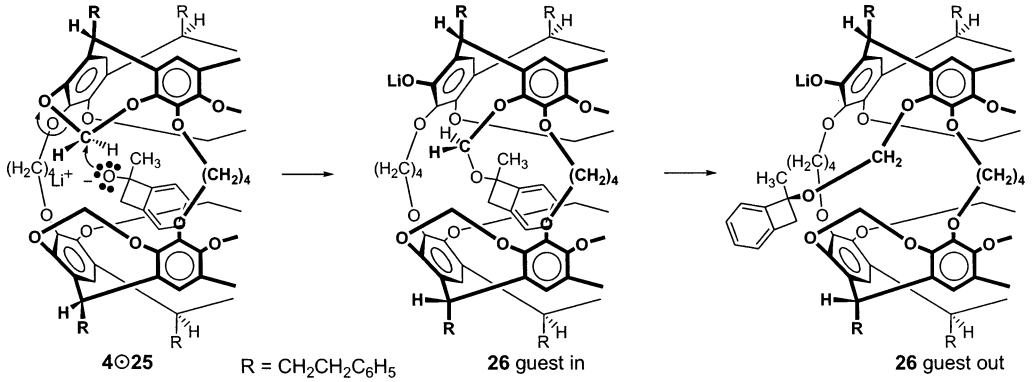

FIGURE 7. Proposed mechanism for the formation of hemicarcerand **24** and *guest inside-out rotation* of intermediate hemicarcerand **26**.

(Figure 7).[33] After the addition of methyllithium to incarcerated **2**, the alcoholate **25** undergoes an inner molecular nucleophilic attack at the acetal carbon of a host spanner. Spaciotemporal effects are probably responsible for the strongly increased nucleophilicity of incarcerated **25**.[34] In the newly formed product **26**, host and guest are linked together via a dioxymethylene linkage. Once **26** is formed, the covalently bound guest can easily rotate from the inner phase through the equatorial host portal to the periphery of the hemicarcerand shell, where the acetal bond is cleaved during the workup to give **24** (Figure 7). Such *inside-out rotation* of a guest that is covalently bound to the portal should be possible at temperatures low enough for constrictive binding to prevent the dissociation of the corresponding hemicarceplex with a nonlinked guest.[7] Alternatively, **26** with the guest inside is cleaved during the workup, followed by dissociation or base-catalyzed opening of the cyclobutenol ring to give **24⊙23**.

Consistent with our interpretation, we observed a higher (**4⊙22** + **4⊙23**)/(**24** + **24⊙23**) ratio of approximately 1:1 (by ^{1}H NMR) when the reaction was quenched after 30 min at room temperature. Although **24⊙23** is always formed as a major product, we never observed formation of **24⊙22**. Either **24⊙22** dissociates during the workup to give empty **24**, preventing its spectroscopic detection, or the base-catalyzed ring-opening of **22** is much faster inside **24** than in the inner phase of **4**. The latter interpretation is reasonable, since the presence of two phenoxides in the molecular shell of deprotonated **24** should allow for a very efficient catalysis of the reaction without the need of a strongly solvated highly polar hydroxide ion to enter the hydrophobic inner phase of **24**. Studies designed to elucidate these mechanisms are currently under way in our laboratories. Interestingly, in this methyllithium addition reaction, we did not observe the formation of diol host **19** (X = H) or host **20** (X = H). On the other hand, **24** was not observed in the alkyllithium additions to **4⊙3**. Thus, small structural changes of the incarcerated lithium alcoholate have a very strong effect on the mode of its innermolecular reactivity.

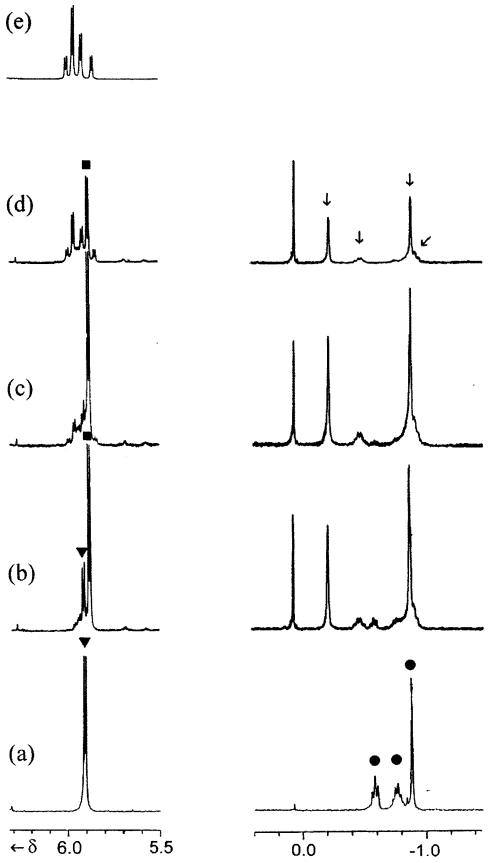

FIGURE 8. Partial ^{1}H NMR spectra ($CDCl_3$, 360 MHz, 22 °C) of the hemicarceplex **4⊙NMP** after 0 min (a), 85 min (b), 13 h (c), and 44 h (d) of exposure to MeLi in THF/ether at 0°C followed by aqueous workup. (e) Partial ^{1}H NMR spectrum ($CDCl_3$, 360 MHz, 22 °C) of hemicarcerand **24** showing the four doublets (ratio 1:3:2:1) which are assigned to the outward-pointing spanner protons. Signals assigned to the outward-pointing spanner protons of **4⊙27** and **4⊙NMP** are marked with filled squares and filled triangles, respectively. Signals assigned to the protons of incarcerated **27** and NMP are marked with arrows and filled circles, respectively.

Methyllithium Addition to 4⊙NMP. Our results in the alkyllithium additions to **4⊙2** and **4⊙3** led us to see if **19** and/or **24** might also be formed from other incarcerated alkoxides. This was the basis for investigating the reaction between **4⊙NMP** and methyllithium. Indeed, addition of MeLi to **4⊙NMP** in THF/ether at 0 °C led to

(32) Wagner, P. J.; Subrahmanyam, D.; Park, B.-S. *J. Am. Chem. Soc.* **1991**, *113*, 709−710.
(33) (a) Kresge, A. J.; Weeks, D. P. *J. Am. Chem. Soc.* **1984**, *106*, 7140−7143. (b) Amyes, T. L.; Jencks, W. P. *J. Am. Chem. Soc.* **1989**, *111*, 7900−7909.
(34) Menger, F. M. *Acc. Chem. Res.* **1993**, *26*, 206−212.

the complete consumption of **4**⊙NMP after 70 h, and **24** was isolated in 70% yield. We followed the progress of this reaction by ^{1}H NMR spectroscopy (Figure 8). Immediately after the MeLi addition, the intensity of the NMP guest signals decreased, while new guest signals at δ −0.21 (s), −0.45 (m), −0.87 (s), and −0.9 (m) appeared. We assign these new signals to guest protons of the 1,2-dimethylpyrrolinol hemicarceplex **4**⊙**27** on the basis of the following observations: (1) The FAB-MS spectrum showed an intensive signal at *m*/*z* 2365 (58%), which is the mass expected for the methyllithium addition product. (2) The newly formed hemicarceplex **4**⊙**27** is stable in solution at room temperature. (3) The guest quantitatively escapes the inner phase of **4** during the column chromatographic workup on silica gel, leaving the empty hemicarcerand. We assume that the acidic silica gel leads to the guest protonation, which facilitates hemicarceplex dissociation.[10] All three observations are consistent with the formation of **4**⊙**27**. After longer reaction times, the intensity of the proton signals of **27** slowly decreased accompanied by the buildup of new signals, which are assigned to host **24** (Figure 8). As discussed earlier for incarcerated lithium alcoholate **21** (Figure 7), we assume that the lithium alcoholate **28** underwent a nucleophilic transacetalization, leading to **29**, which is hydrolyzed to give **24** during the workup.

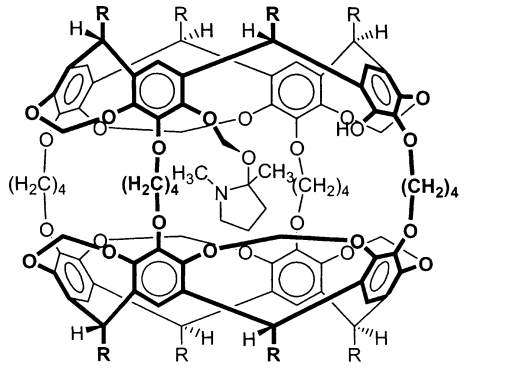

29 R = $CH_2CH_2C_6H_5$

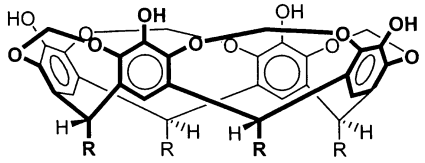

30

The efficient synthesis of **4**⊙NMP, which can be prepared in high yield (40−45%) from cavitand **30**,[10] and the absence of other cleavage products such as **19** and **20** make the MeLi addition to **4**⊙NMP a fast method for the preparation of empty hemicarcerand **4** or host **24**. Hemicarcerand **24** should be a very useful intermediate for the incarceration of guests that are too large to pass through an equatorial portal of **4** and for the incorporation of catalytic functional groups into the host shell.

Correlation between Reactivity and Guest Conformation. The observed inner-phase guest reactivity decreased in the order **3** ≫ **2** > **1** in the through-shell methyllithium additions and in the order **3** ≈ **2** > **1** in the through-shell borane reductions. Why are **2** and **3** more reactive than benzaldehyde **1** in the inner phase as compared to the liquid bulk phase? The selectivity in the MeLi addition to incarcerated **3** and also the fact that the addition takes place at −78 °C suggest that the reacting carbonyl group is located close to an equatorially located entryway of **4**. To determine the orientations of the guests **1**−**3** in the inner phase of host **4**, we undertook X-ray crystal studies of the three hemicarceplexes. All three complexes were crystallized by slow evaporation

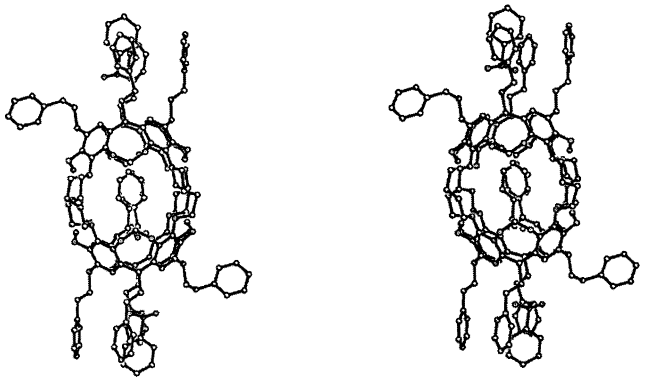

FIGURE 9. Stereoview of the hemicarceplex **4**⊙benzaldehyde·2nitrobenzene. All H atoms are omitted; two of the four disordered benzaldehyde guest positions are shown (the other two are generated by the center of symmetry).

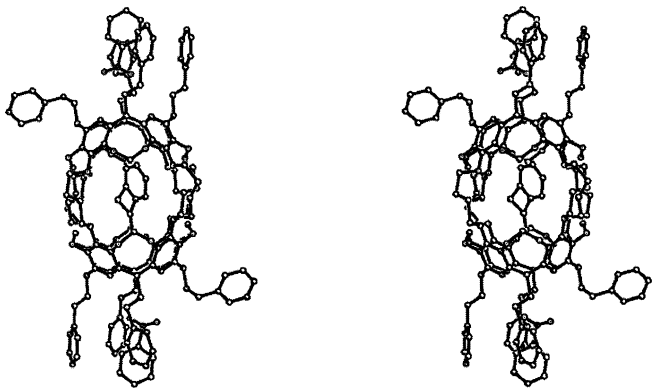

FIGURE 10. Stereoview of the hemicarceplex **4**⊙benzocyclobutenone·2nitrobenzene. All H atoms are omitted; one of the two disordered benzocyclobutenone guest positions is shown (the other is generated by the center of symmetry).

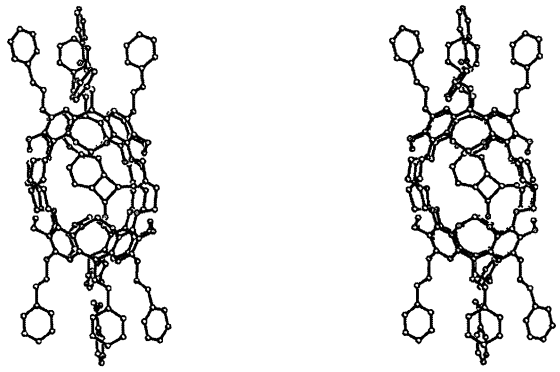

FIGURE 11. Stereoview of the hemicarceplex **4**⊙benzocyclobutenedione·2nitrobenzene. All H atoms are omitted; one of the two disordered benzocyclobutenedione guest positions is shown (the other is generated by the center of symmetry).

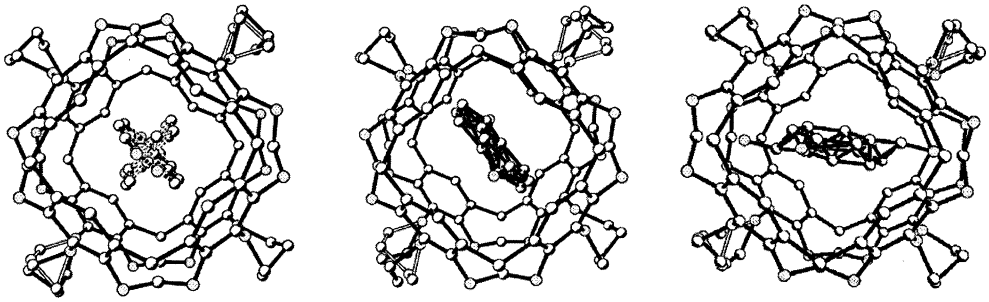

FIGURE 12. Top views of **4**⊙**1**, **4**⊙**2**, and **4**⊙**3**, left to right. "Feet", nitrobenzene, and all H atoms are removed for clarity. Disordered $-O(CH_2)_4O-$ bridging linkers are shown at the bottom left and top right. The entire guest model is shown (site occupancy 1.0).

CHART 2. Hemicarcerand-Induced Upfield Shifts of Guest Protons in 4⊙1, 4⊙2, and 4⊙3

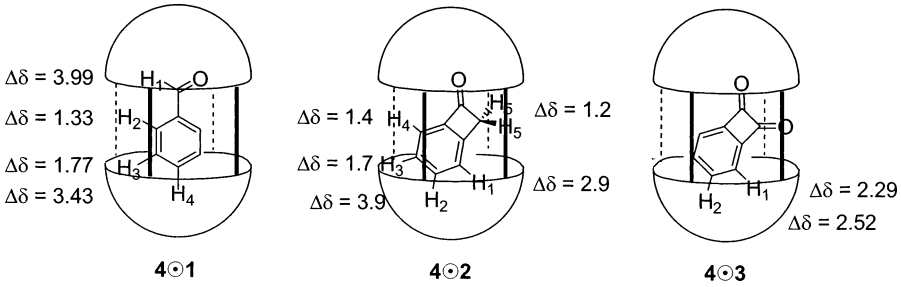

from chloroform/nitrobenzene, and all three are approximately isomorphous with other complexes of the same host crystallized from this solvent mixture.[19] In the crystals, **4** lies on a center of symmetry, requiring disorder in the noncentrosymmetric guests. One molecule of nitrobenzene is located in each "foot" region; these regions are formed by four $-CH_2CH_2C_6H_5$ groups that help to make the host soluble in nonpolar solvents. In **4**⊙**1** (Figure 9), the final refinement model includes two guest molecules at 0.25 occupancy, roughly orthogonal to each other. In **4**⊙**2** and **4**⊙**3** (Figures 10 and 11), one molecule of guest was refined at 0.5 occupancy. The additional guest moieties generated by the center of symmetry bring the site occupancies to 1.0 in each complex. Though the guests and bridges are disordered, it is clear that the carbonyl O atom lies in a polar cap of the host in each complex, while the second carbonyl O in **4**⊙**3** is in a portal, between bridges (Figures 9−11).

Host **4** is able to adjust to the dimensions and chemical nature of its guests,[19] and **4**⊙**1**, **4**⊙**2**, and **4**⊙**3** demonstrate this adaptability in two ways. First, the two partial-occupancy, planar molecules of **1** in the complex are aligned between bridges, with the shortest guest-to-host distances being H(guest)···bridgehead O(host), 2.3−2.6 Å. In **4**⊙**2** the guest is also aligned between bridges, and the shortest guest-to-host distances are H(guest)··· bridgehead O(host), 1.9−2.4 Å, and O(guest)···spanner H(host), 2.8 Å. In contrast, **3** in its complex is aligned between portals, with the shortest guest-to-host distance being O(guest)···spanner H(host), 2.2−2.3 Å. Second, though the two hemispheres of host **4** may twist with respect to each other to accommodate guests,[19] in **4**⊙**1**, **4**⊙**2**, and **4**⊙**3**, as in all other examples of the isomorphous nitrobenzene solvate series, they are eclipsed. However, the distances between the planes of the bridgehead O atoms of **4** in connected hemispheres differ (3.77 Å in **4**⊙**1**, 3.87 Å in **4**⊙**2**, and 3.99 Å in **4**⊙**3**), showing the flexibility of the $-O(CH_2)_4O-$ linkers. Figure 12 shows the alignment of the guest molecules in the host cavity.

FIGURE 13. Energy-minimized structure of hemicarceplex **4**⊙**2** (MM2 force field, Macromodel).[35,36] Phenethyl feet and host hydrogen atoms have been omitted. Atom coloring is as follows: O, red; host C, gray; guest C, black; H, white.

Since the crystal study of **4**⊙**2** gave ambiguous starting positions for guest atoms, we determined the lowest-energy orientation by molecular mechanics calculations (Figure 13). In the calculated structure the carbonyl group is aligned with the host's polar D_4 axis and partially protrudes into a polar cap of **4**. When the calculated internal coordinates for the guest were applied to the refinement model in the crystal structure, the orientation of the guest was confirmed (Figures 10 and 12).

The solid-state inner-phase orientation of **1** and **3** and the predicted orientations of **2** are consistent with the observed host-induced upfield shift of the guest protons of **1**−**3** (Chart 2). Protons that are preferentially located in a polar cap are shielded more strongly in comparison to protons that are located in the central part of the inner

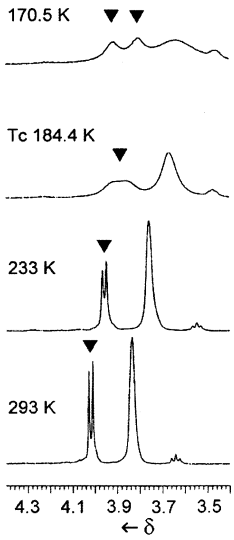

FIGURE 14. Partial ^{1}H NMR (400 MHz, $CD_2Cl_2/CDCl_3$ (7:1)) of **4**⊙**1** at different temperatures. Signals assigned to the inward-pointing spanner protons of **4** are marked with filled triangles.

phase.[7,8,19,20,28] Thus, very similar guest orientations are expected in solution and allow us to rationalize the observed order of guest reactivity.

In **4**⊙**3**, one guest carbonyl is favorably aligned for efficient through-shell reaction without the necessity of guest reorientation, which explains the high reactivity of **3** even at −78 °C. On the other hand, in **4**⊙**1** and **4**⊙**2** a through-shell reaction requires **1** and **2** to tilt considerably away from their favored orientation, which would explain their low reactivity toward MeLi as compared to that of **4**⊙**3**. We suggest that the higher reactivity of **2** as compared to **1** is related to the ease of adapting a reactive orientation in which the carbonyl group is pointing toward a portal of **4**, and that the energy is smaller for **2**. A qualitative measure for this energy might be the barrier for guest rotation $\Delta G^{\ddagger}$ around the equatorial C_2 axis of **4**. We determined $\Delta G^{\ddagger}$ for **1** by low-temperature ^{1}H NMR studies. At 170.5 K, two sets of inward-pointing hydrogen resonances are observed as a consequence of the reduction of the host symmetry in the limit of slow guest rotation around an equatorially located host C_2 axis (Figure 14, top). These multiplets coalesce at T_c = 184.4 K (Figure 14, middle), from which we calculated $\Delta G^{\ddagger}_{184.4K} = 8.9 \pm 0.3$ kcal/mol.[37]

The inner-phase rotation of **2**, on the other hand, could not be frozen out in $(CD_2)_4O$ at 164 K, and therefore, we predict a lower barrier as compared to that of **1**, consistent with our interpretation of the through-shell reactivity of **1** and **2**. The higher rotational barrier $\Delta G^{\ddagger}$ of **1** is surprising in light of the larger size of **2**. The restriction of rotational mobility of the C(1)−$C_{carbonyl}$ bond of **1** in the transition-state region for the inner-phase guest rotation leads to an unfavorable internal entropy contribution and might contribute to the higher $\Delta G^{\ddagger}$ of **1** (Chart 3).

CHART 3. Restricted Internal Rotation of Incarcerated Benzaldehyde in Its Low-Energy and High-Energy Orientations

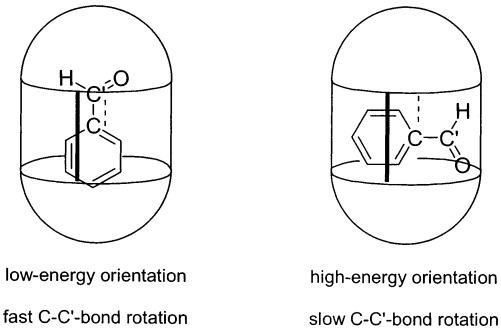

Hence, guest reactivity is not just a function of the reactive group location with respect to the host's equatorial portals, but is also very strongly correlated to the guest mobility and the probability that the reactive group will be exposed to an equatorial portal, which is required for a through-shell reaction with a bulk-phase reactant.

Conclusions

Through-shell and inner-phase chemistries clearly differ from "conventional" chemistry in the bulk phase with respect to their rates and their selectivity. In accordance with earlier results,[9,10] the inner-phase and through-shell reactions reported here show the following characteristic features:

(1) Functional groups of the guest that are located in the inner cavity of a host's polar cavitand are less reactive than those exposed to an equatorial portal, which have the potential for high through-shell reactivity.

(2) The reactivity of bulk-phase reactants is largely influenced by their size and shape relative to the size and shape of the host's equatorial portals.

(3) If functional groups are protected in the guest's most favorable orientation, reactivity depends on the inner-phase rotational mobility of the guest.

Furthermore, our studies on the through-shell alkyllithium additions to **1**−**3** and NMP show that the basicity and nucleophilicity of incarcerated lithium alcoholates strongly exceed by several orders of magnitude those of bulk-phase alcoholates, resulting in efficient innermolecular elimination or nucleophilic transacetalization reactions and the formation of hemicarcerands with one extended portal in the host shell. In these innermolecular reactions, small structural changes of the guest have a sound effect on the reaction mode. Especially noteworthy is the highly efficient formation of host **24** via the addition of methyllithium to **4**⊙NMP. This reaction should be very useful for the attachment of a single tether to a hemicarcerand, which is desirable for hemicarcerand immobilization. Studies in this direction are currently under way.

Experimental Section

All reactions were conducted under argon unless otherwise stated. Tetrahydrofuran was freshly distilled from benzophe-

(35) (a) Goodman, J. M.; Still, W. C. *J. Comput. Chem.* **1991**, *12*, 1110−1117. (b) Allinger, N. L. *J. Am. Chem. Soc.* **1977**, *99*, 8127−8134. (c) Still, W. C.; Tempczyk, A.; Hawley, R. C.; Hendrickson, T. *J. Am. Chem. Soc.* **1990**, *112*, 6127−6129.

(36) (a) Houk, K. N.; Nakamura, K.; Sheu, C.; Keating, A. E. *Science* **1996**, *273*, 627−629. (b) Nakamura, K.; Houk, K. N. *J. Am. Chem. Soc.* **1995**, *117*, 1853−1854. (c) Sheu, C.; Houk, K. N. *J. Am. Chem. Soc.* **1996**, *118*, 8056−8070.

(37) Günther, H., Ed. *NMR-Spektroskopie*, 3rd ed.; Georg Thieme Verlag: Stuttgart, Germany, 1992; pp 310−312.

none ketyl just prior to use. ^{1}H NMR spectra and ^{13}C NMR spectra were recorded at the indicated frequency. FAB mass spectra were determined with 3-nitrobenzyl alcohol matrix. FT-IR spectra were obtained in $CHCl_3$ solution. CHN elementary analyses were obtained from Desert Analytics, Tucson, AZ. Gravity chromatography was performed on silica gel (70−230 mesh). Thin-layer chromatography involved polyethylene-backed plates (silica gel, 0.25 mm). Preparative thin-layer chromatography involved glass-backed plates (silica gel 60, 0.5 or 1 mm). Compounds **2**,[38] **3**,[38,39] **14**,[40] and **30**[10] were synthesized according to literature procedures.

General Procedure for the Synthesis of Hemicarceplexes 4⊙Guest and 24⊙Guest (Procedure A). A 1 mol equiv sample of hemicarcerand **4** (or **24**) and 50 mol equiv of the guest were sealed under argon in a glass ampule and were heated for the specified time at the specified temperature. After the reaction mixture had cooled to room temperature, the ampule was opened. The reaction mixture was poured into a 10-fold volume of methanol. If the free guest was a solid, the content of the ampule was dissolved in a minimum volume of $CHCl_3$, which was poured into the 10-fold volume of methanol. The precipitated crude hemicarceplex was collected on a glass sinter (pore size 10−15 μm), washed with methanol, and dried at high vacuum. Purification by column chromatography on SiO_2 with CH_2Cl_2 as the mobile phase or by preparative TLC on SiO_2 with $CHCl_3$ as the mobile phase gave the pure hemicarceplex **4**⊙guest (**24**⊙guest).

Benzaldehyde Hemicarceplex 4⊙1. Application of procedure A (5 days, 170 °C, preparative TLC on SiO_2 (0.5 mm)) gave **4⊙1** (95% yield) as a white powder. ^{1}H NMR (360 MHz, $CDCl_3$, 25 °C): δ 7.16−7.26 (m, 40H), 6.98 (s, 8H), 6.58 (s, 1H, guest-C*H*O), 6.55 (d, 2H, guest-H), 5.75 (t, 2H, guest-H), 5.66 (d, 8H), 4.85 (t, 8H), 4.05 (d, 8H), 3.88 (br s, 16H), 3.64 (t, 1H, guest-H), 2.47−2.75 (m, 32H), 1.90 (br s, 16H). FAB-MS: *m*/*z* [M + H]$^+$, 2356 (100); [M − **1** + H]$^+$, 2250 (43). Anal. Calcd for $C_{151}H_{142}O_{25}$: C, 76.96; H, 6.07. Found: C, 76.89; H, 6.10.

Benzocyclobutenone Hemicarceplex 4⊙2. Application of procedure A (8 days, 150 °C, column chromatography on SiO_2) gave **4⊙2** (80% yield) as a white powder. ^{1}H NMR (400 MHz, $CDCl_3$, 25 °C): δ 7.16−7.26 (m, 40H), 6.96 (s, 8H), 6.17 (d, 1H, guest-H), 5.73 (t, 1H, guest-H), 5.62 (d, 8H), 4.85 (t, 8H), 4.67 (d, 1H, guest-H), 4.08 (d, 8H), 3.92 (br s, 16H), 3.62 (t, 1H, guest-H), (s, 2H, guest-CH_2), 2.47−2.75 (m, 32H), 1.88 (br s, 16H). FAB-MS: *m*/*z* [M + H]$^+$, 2368.4 (100); [M − **2** + H]$^+$, 2250 (43). Anal. Calcd for $C_{152}H_{142}O_{25}$: C, 77.04; H, 6.04. Found: C, 77.27; H, 6.01.

Benzocyclobutenedione Hemicarceplex 4⊙3.[8] Application of procedure A (4 days, 145 °C, column chromatography on SiO_2) gave **4⊙3** (30% yield) as a slightly yellow powder. ^{1}H NMR (500 MHz, $CDCl_3$, 25 °C): δ 7.16−7.27 (m, 40H), 6.96 (s, 8H), 5.76 (dd, 2H, guest-H), 5.62 (d, 8H), 5.25 (dd, 2H, guest-H), 4.86 (t, 8H), 4.10 (d, 8H), 3.96 (br s, 16H), 2.47−2.75 (m, 32H), 1.92 (br s, 16H). FT-IR ($CHCl_3$, 25 °C, cm^{-1}): ν(CO) 1782. FAB-MS: *m*/*z* [M + H]$^+$, 2382.9 (100); [M − **3** + H]$^+$, 2250.8 (39). Anal. Calcd for $C_{152}H_{140}O_{26}$: C, 76.62; H, 5.92. Found: C, 76.87; H, 5.77.

Benzyl Alcohol Hemicarceplex 4⊙5. Application of procedure A (70 h, 170 °C, preparative TLC on SiO_2 (0.5 mm)) gave **4⊙5** (95% yield) as a white powder. ^{1}H NMR (360 MHz, $CDCl_3$, 25 °C): δ 7.1−7.4 (m, 40H), 6.94 (s, 8H), 6.09 (d, 2H, guest-H), 5.66 (d, 8H), 5.37 (t, 2H, guest-H), 4.86 (t, 8H), 4.71 (br s, 1H, guest-H), 4.20 (d, 8H), 3.89 (br s, 16H), 3.24 (t, 1H, guest-H), 2.47−2.75 (m, 32H), 1.91 (br s, 16H), 1.75 (d, 2H, guest-C*H*$_2$), −2.59 (t, 1H, guest-H). FAB-MS: *m*/*z* [M + H]$^+$, 2358 (37); [M − CH_2O + H]$^+$, 2328 (100); [M − **5** + H]$^+$, 2250 (38). Anal. Calcd for $C_{151}H_{144}O_{25}$: C, 76.89; H, 6.15. Found: C, 76.91; H, 6.05.

1-Phenylethanol Hemicarceplex 4⊙12. Application of procedure A (70 h, 170 °C, preparative TLC on SiO_2 (0.5 mm)) gave **4⊙12** (95% yield) as a white powder. ^{1}H NMR (360 MHz, $CDCl_3$, 25 °C): δ 7.16−7.26 (m, 40H), 6.91 (br s, 8H), 6.17 (d, 2H, guest-H), 5.66 (d, 8H), 5.18 (t, 2H, guest-H), 4.84 (t, 8H), 4.6−3.9 (3 v br s, 16 H), 3.85 (t, 8H), 3.51 (t, 1H, guest-H), 3.05 (q, 1H, guest-C*H*CH_2OH), 2.47−2.75 (m, 32H), 2.1−1.8 (m, 16H), −2.42 (d, 3H, guest-CH_3). FAB-MS: *m*/*z* [M + H]$^+$, 2371 (25); [M − **12** + H]$^+$, 2251 (85). Anal. Calcd for $C_{152}H_{146}O_{25}$: C, 76.94; H, 6.20. Found: C, 76.88; H, 6.20.

7-Methylphthalide Hemicarceplex 24⊙14. Application of procedure A (36 h, 185 °C, preparative TLC on SiO_2 (0.5 mm)) gave **24⊙14** (70% yield) as a white powder. ^{1}H NMR (400 MHz, $CDCl_3$, 60 °C): δ 7.83 (br s, 1H, O*H*), 7.43 (br s, 1H, O*H*), 7.30−7.10 (m, 40H, C_6H_5), 7.07 (s, 1H, Ar*H* on bowl), 7.00 (s, 1H, Ar*H* on bowl), 6.96 (s, 1H, Ar*H* on bowl), 6.94 (s, 1H, Ar*H* on bowl), 6.93 (s, 1H, Ar*H* on bowl), 6.92 (s, 1H, Ar*H* on bowl), 6.89 (s, 1H, Ar*H* on bowl), 6.86 (s, 1H, Ar*H* on bowl), 6.57 (d, 1H, guest), 6.26 (t, 1H, guest), 5.89 (d, 1H, OC*H*$_2$O outer), 5.86 (d, 1H, OC*H*$_2$O outer), 5.85 (d, 1H, OC*H*$_2$O outer), 5.78 (d, 1H, OC*H*$_2$O outer), 5.54 (d, 1H, OC*H*$_2$O outer), 5.47 (d, 1H, guest), 5.42 (d, 1H, OC*H*$_2$O outer), 5.42 (d, 1H, OC*H*$_2$O inner), 5.27 (d, 1H, OC*H*$_2$O outer), 5.07 (t, 1H, C*H* methine), 5.02 (t, 1H, C*H* methine), 4.96 (t, 1H, C*H* methine), 4.81 (t, 1H, C*H* methine), 4.79 (t, 1H, C*H* methine), 4.66 (t, 1H, C*H* methine), 4.63 (t, 1H, C*H* methine), 4.62 (t, 1H, C*H* methine,), 4.62 (d, 1H, OC*H*$_2$O inner), 4.56 (d, 1H, OC*H*$_2$O inner), 3.87 (d, 1H, OC*H*$_2$O inner), 3.84 (d, 1H, OC*H*$_2$O inner), 4.22−3.76 (m, 15H, OC*H*$_2$CH$_2$), 3.76 (t, 1H, guest), 3.63 (m, 1H, OC*H*$_2$-CH$_2$), 3.62 (q, 1H, C*H*CH$_3$, guest), 3.25 (br s, 1H, OC*H*$_2$O inner), 3.12 (br s, 1H, OC*H*$_2$O inner), 2.78−2.35 (m, 32H, C*H*$_2$C*H*$_2$Ph), 2.1−1.6 (m, 16H, OC*H*$_2$CH$_2$), −2.01 (d, 3H, C*H*$_3$, guest). FAB-MS: *m*/*z* [M + H]$^+$, 2384.6 (50); [M − **23** + H]$^+$, 2238.1 (100). Anal. Calcd for $C_{152}H_{144}O_{26}$: C, 76.49; H, 6.08. Found: C, 76.70; H, 6.13.

2-Methylacetophenone Hemicarceplex 24⊙23. Application of procedure A (70 h, 185 °C, preparative TLC on SiO_2 (0.5 mm)) gave **24⊙23** (65% yield) as a white powder. ^{1}H NMR (400 MHz, $CDCl_3$, 25 °C): δ 7.10−7.30 (m, 40H, C_6H_5), 7.01 (s, 2H, Ar*H* on bowl), 6.92 (s, 2H, Ar*H* on bowl), 6.91 (s, 2H, Ar*H* on bowl), 6.86 (s, 2H, Ar*H* on bowl), 6.77 (s, 2H, O*H*, disappears upon D_2O addition), 6.24 (d, 1H, guest-H), 5.93 (d, 1H, OC*H*$_2$O outer), 5.89 (d, 1H, OC*H*$_2$O outer), 5.82 (d, 1H, OC*H*$_2$O outer), 5.73 (tb, 1H, guest-H), 5.49 (d, 1H, OC*H*$_2$O outer), 5.42 (d, 1H, OC*H*$_2$O outer), 5.00 (t, 1H, C*H* methine), 4.96 (t, 2 H, C*H* methine), 4.92 (d, 2 H, OC*H*$_2$O inner), 4.73 (t, 2 H, C*H* methine), 4.61 (t, 1H, C*H* methine), 4.57−4.65 (m, 5 H, OC*H*$_2$O inner, C*H* methine), 4.55 (br d, 1H, guest-H), 3.8−4.24 (m, 14 H, OC*H*$_2$CH$_2$), 3.82 (d, 2 H, OC*H*$_2$O inner), 3.7−3.78 (m, 2H, OC*H*$_2$CH$_2$), 3.66 (t, 1H, guest-H), 3.44 (d, 2 H, OC*H*$_2$O inner), 2.4−2.8 (m, 32H, C*H*$_2$C*H*$_2$Ph), 1.75−2.0 (m, 16H, OCH$_2$C*H*$_2$), 1.64 (s, 3H, guest-CH_3), −1.29 (s, 3H, guest-CH_3). FAB-MS: *m*/*z* [M + H]$^+$, 2371 (50); [M − **23** + H]$^+$, 2238 (100). Anal. Calcd for $C_{152}H_{146}O_{25}$: C, 76.94; H, 6.20. Found: C, 76.97; H, 5.97.

2-Methylacetophenone Hemicarceplex 4⊙23 (Procedure B). Hemicarceplex **24⊙23** (18 mg, 7.6 μmol), anhydrous potassium carbonate (500 mg), excess $BrCH_2Cl$ (1 mL), and degassed DMF (4 mL) were stirred for 48 h at 60 °C under argon. The cooled reaction mixture was poured into methanol/water (1:1, 50 mL). The precipitate was filtered off, washed with water and methanol, and dried at high vacuum. Preparative TLC (SiO_2, mobile phase CH_2Cl_2) provided 12 mg of hemicarceplex **24⊙23** as a white powder (67% yield). ^{1}H NMR (360 MHz, $CDCl_3$, 25 °C): δ 7.1−7.3 (m, 40H), 6.92 (s, 8H), 6.63 (t, 1H, guest-H), 6.49 (d, 1H, guest-H), 5.66 (d, 8H), 4.85 (t, 8H), 4.45 (d, 1H, guest-H), 4.24 (br s, 8H), 3.97 (br s, 16H), 3.63 (t, 1H, guest-H), 2.45−2.75 (m, 32H), 1.84 (br s, 19H), −1.40 (s, 3H, guest-CH_3). FT-IR ($CHCl_3$, 25 °C, cm^{-1}): ν(CO) 1696. FAB-MS: *m*/*z* [M + H]$^+$, 2383 (63); [M − **23** + H]$^+$, 2250

(38) Dürr, H.; Nickels, H.; Pacala, L. A.; Jones, M., Jr. *J. Org. Chem.* **1980**, *45*, 973−980.
(39) Cava, M. P.; Mangold, D.; Muth, K. *J. Org. Chem.* **1964**, *29*, 2947−2948.
(40) Canonne, P.; Plamondon, J.; Akssira, M. *Tetrahedron* **1988**, *44*, 2903−2912.

(100). Anal. Calcd for $C_{153}H_{146}O_{25}$: C, 76.99; H, 6.25. Found: C, 77.36; H, 6.22.

7-Methylphthalide Hemicarceplex 4⊙14. Application of procedure B on hemicarceplex **24⊙14** gave hemicarceplex **4⊙14** as a white powder. ^{1}H NMR (400 MHz, $CDCl_3$, 25 °C): δ 7.16−7.26 (m, 40H), 6.91 (s, 8H), 6.81 (d, 1H, guest-H), 6.75 (t, 1H, guest-H), 5.63 (br s, 8H), 5.29 (d, 1H, guest-H), 4.87 (t, 8H), 4.32 (v br s, 8 H), 3.9−4.1 (m, 16H), 3.70 (q, 1H, guest-C*H*CH_3O), 3.70 (t, 1H, guest-H), 2.47−2.75 (m, 32H), 1.84 (br s, 16H), −2.15 (d, 3H, guest-CH_3). FT-IR ($CHCl_3$, 25°C, cm^{-1}): ν(CO) 1781. FAB-MS: *m*/*z* $[M + H]^+$, 2398.1 (100); $[M - \mathbf{14} + H]^+$, 2249.5 (85). Anal. Calcd for $C_{153}H_{144}O_{26}$: C, 76.61; H, 6.05. Found: C, 76.73; H, 5.77.

1-Methyl-2-pyrrolidinone Hemicarceplex 4⊙NMP.[20] A solution of **30** (2 g, 1.97 mmol),[10] butane-1,4-diol dimesylate (2 g, 8.13 mmol), and anhydrous Cs_2CO_3 (10 g) in degassed NMP (500 mL) was stirred for 24 h at room temperature under argon. Butane-1,4-diol dimesylate (2 g, 8.13 mmol) was added, and stirring was continued for 24 h at room temperature and for 48 h at 60 °C. The reaction mixture was cooled to room temperature and poured into water/brine (1:1, 4 L). The precipitate was filtered off, washed with water (500 mL) and methanol (100 mL), and redissolved in $CHCl_3$ (20 mL). The $CHCl_3$ solution was dropwise added to vigorously stirred methanol (200 mL). The precipitated crude product was filtered off, washed with methanol (10 mL), and dried at high vacuum overnight. The crude product was purified by column chromatography on SiO_2 with $CHCl_3$ as the mobile phase to give **4⊙**NMP as a white solid (1.02 g, 44% yield). ^{1}H NMR (360 MHz, $CDCl_3$, 25 °C): δ 7.25−7.12 (m, 40H), 6.86 (s, 8H), 5.81 (d, 8H), 4.85 (t, 8H), 4.32 (d, 8H), 3.95 (br s, 16H), 2.40−2.73 (m, 32H), 1.99 (m, 18H), −0.58 (t, 2H, guest), −0.76 (m, 2H, guest), −0.88 (s, 3H, guest).

Borane Reduction of 4⊙1 (Procedure C). A solution of BH_3·THF in THF (1 M, 5 mL) was added under argon to of **4⊙1** (12 mg, 5.1 μmol). The solution was refluxed for 16 h, cooled to room temperature, and quenched by slow syringe addition of water (5 mL). $CHCl_3$ (10 mL) was added. Both layers were separated, and the aqueous layer was extracted twice with $CHCl_3$ (5 mL). The combined organic layers were dried over $MgSO_4$ and concentrated to 1 mL. Methanol (10 mL) was added. The precipitate was filtered off, washed with methanol, and dried at the high vacuum for 10 h to yield a hemicarceplex mixture (12 mg), whose composition was determined by the intensities of selected ^{1}H NMR signals of all incarcerated guest molecules. The mixture contained 13% **4⊙5**, 13% **4**⊙THF,[19] and 67% **4⊙1**.

Borane Reduction of 4⊙2. Application of procedure C to hemicarceplex **4⊙2** (reflux, 40 h) gave a crude hemicarceplex mixture containing 85% **4**⊙benzocyclobutenol (**4⊙6**) as determined by ^{1}H NMR. Purification by preparative TLC on SiO_2 with CH_2Cl_2 as the mobile phase gave **4⊙6** as a white solid. ^{1}H NMR (400 MHz, $CDCl_3$, 25 °C): δ 7.15−7.3 (m, 40H), 6.95 (s, 8H), 6.07 (t, 1H, guest-H), 5.64 (d, 8H), 5.54 (d, 1H, guest-H), 4.85 (t, 8H), 4.31 (m, 1H, guest-H), 4.26 (d, 8H), 4.00 (m, 8H), 3.86 (m, 8H), 2.47−2.75 (m, 32H), 2.65 (d, 1H, guest-H), 1.85−1.95 (m, 16H), 1.26 (s, 1H, guest-O*H*), 1.01 (dd, 1H, guest-*H*), 0.9 (dd, 1H, guest-*H*). FAB-MS: *m*/*z* $[M + H]^+$, 2370.1 (37); $[M - CH_2O + H]^+$, 2340.3 (100); $(M - \mathbf{6} + H]^+$, 2249.6 (22). Anal. Calcd for $C_{152}H_{144}O_{25}$: C, 77.01; H, 6.15. Found: C, 77.31; H, 5.97.

Borane Reduction of 4⊙3. Application of procedure C to hemicarceplex **4⊙3** (reflux, 49 h) gave a crude hemicarceplex mixture containing 90% hemicarceplex **4.**8-hydroxybenzocyclobutene-7-one (**4⊙7**), 4% **4**⊙THF,[19] and 6% **4⊙3** as determined by ^{1}H NMR spectroscopy. Purification by preparative TLC on SiO_2 with CH_2Cl_2 gave **4⊙7** as a white solid (81% isolated yield). ^{1}H NMR (500 MHz, $CDCl_3$, 25 °C): δ 7.13−7.3 (m, 40H, C_6H_5), 7.10 (t, 1H, guest-H) 7.05 (br s, 8H, Ar*H* of bowl), 6.63 (d, 1H, guest-H), 5.68 (d, 8H, OCH_2O outer), 5.10 (d, 1H, guest-H), 4.91 (t, 8H, C*H* methine), 4.24 (d, 8H, OCH_2O inner), 4.08 (br s, 8H, OCH_2CH_2), 4.04 (t, 1H, guest-H), 3.99 (br s, 8H, OCH_2CH_2), 3.61 (t, 1H, guest-H), 2.46−2.78 (m, 32H, CH_2CH_2Ph), 1.94 (br s, 16H, OCH_2CH_2), 1.32 (v br s, 1H, guest-H). ^{13}C NMR (125.6 MHz, $CDCl_3$, 25 °C): δ 186.8 (guest), 155.7 (guest), 148.6, 146.3 (guest), 143.8, 141.9, 138.7, 132.3 (guest), 130.6 (guest), 128.6, 128.5, 126.0, 122.1 (guest), 119.4 (guest), 114.3, 99.0, 85.6 (guest), 72.2, 37.2, 34.6, 32.6, 27.7. FAB-MS (NBA-matrix): *m*/*z* $[M + H]^+$, 2384 (100); $[M - \mathbf{7} + H]^+$, 2250 (42). Anal. Calcd for $C_{152}H_{142}O_{26}$: C, 76.56; H, 6.00. Found: C, 76.33; H, 6.05.

Hemicarceplex 4⊙9 via Borane Reduction of 4⊙7. Application of procedure C to hemicarceplex **4⊙7** (reflux, 90 h, preparative TLC on SiO_2 with CH_2Cl_2 as the mobile phase) gave hemicarceplex **4⊙9** (85% yield). ^{1}H NMR (500 MHz, $(CD_2)_4O$/5% D_2O, 25 °C): δ 7.13−7.3 (m, 40H, C_6H_5), 7.01 (br s, 8H, Ar*H* on bowl), 6.54 (dd, 2H, guest-H), 5.68 (d, 8H, OCH_2O outer), 4.92 (s, 2H, guest-H), 4.82 (t, 8H, C*H* methine), 3.9−4.7 (v br s, 8H, OCH_2O inner), 4.00 (br s, 16H, OCH_2-CH_2), 3.92 (dd, 2H, guest-H), 2.47−2.70 (m, 32H, CH_2CH_2Ph), 1.91 (br s, 16H, OCH_2CH_2), −0.6 to −0.1 (v br s, 1H, B*H*). ^{13}C NMR (125.6 MHz, $CDCl_3$, 25 °C): δ 148.2, 145.7 (guest), 144.4, 141.8, 138.6, 128.6, 128.4, 127.7 (guest), 126.0, 122.7 (guest), 114.0, 97.5, 78.0 (guest), 71.8, 37.1, 34.5, 32.5, 29.7, 28.1. ^{11}B NMR (160.5 MHz, $CDCl_3$, 25 °C): δ 28.3. FT-IR ($CHCl_3$, 25 °C, cm^{-1}): ν(B−H) 2655. FAB-MS (NBA-matrix): *m*/*z* ([M + H]$^+$, 2395.7 (75); $[M - \mathbf{9} + H]^+$, 2249.4 (100). Anal. Calcd for C_{152} $H_{143}O_{26}B$: C, 76.18; H, 6.01. Found: C, 76.23; H, 6.00.

Hydrolysis of Hemicarceplex 4⊙9. Hemicarceplex **4⊙9** (10 mg, 4.2 μmol) dissolved in water-saturated $CDCl_3$ was left standing at room temperature in a NMR tube. The guest slowly hydrolyzed within 3 weeks to yield **4**⊙*cis*-benzocyclobutene-7,8-diol (**4⊙10**). Purification by preparative TLC on SiO_2 with $CHCl_3$ as the mobile phase gave **4⊙10** as a white solid (9 mg, 90% yield). ^{1}H NMR (500 MHz, $CDCl_3$, 25 °C): δ 7.16−7.3 (m, 40H, C_6H_5), 6.95 (s, 8H, Ar*H* on bowl), 5.64 (d, 8H, OCH_2O outer), 5.08 (m, 2H, guest-H), 5.00 (m, 2H, guest-H), 4.84 (t, 8H, C*H* methine), 4.33 (d, 8H, OCH_2O inner), 3.95 (br s, 16H, OCH_2CH_2), 3.76 (d, 2H, guest-H), 2.47−2.73 (m, 32H, CH_2CH_2Ph), 1.90 (br s, 16H, OCH_2CH_2), 1.41 (d, 2H, guest-H). ^{13}C NMR (125.6 MHz, $CDCl_3$, 25 °C) δ 148.4, 145.7 (guest), 144.0, 141.8, 138.7, 128.6, 128.4, 127.9 (guest), 126.0, 121.8 (guest), 113.9, 98.9, 83.0 (guest), 73.0 (guest), 72.3, 37.1, 34.5, 32.6, 29.7, 27.7. FAB-MS: *m*/*z* $[M + H]^+$, 2386 (100). Anal. Calcd for $C_{152}H_{144}O_{26}$: C, 76.49; H, 6.08. Found: C, 76.81; H, 6.15.

Methyllithium Addition to 4⊙1 (Procedure D). Hemicarceplex **4⊙1** (55 mg, 23.3 μmol) was dissolved in dry THF (5 mL) under argon. MeLi in diethyl ether (1.4 M, 4 mL) was added, and the mixture was stirred for 8 h, cooled to −78 °C, and quenched with saturated NH_4Cl solution (5 mL). The two phases were separated, and the aqueous layer was extracted with chloroform (10 mL). The combined organic layers were dried over $MgSO_4$ and concentrated. The crude product mixture was purified by preparative TLC on SiO_2 with $CHCl_3$/5% EtOAc as the mobile phase to yield 64% recovered **4⊙1** (35 mg) and 11% **4**⊙1-phenylethanol (**4⊙12**) (6 mg).

Methyllithium Addition to 4⊙3 at −78 °C. Application of procedure D to hemicarceplex **4⊙3** (THF/ether (8:5), −78 °C, 30 h) and purification of the crude products by preparative TLC on SiO_2 with CH_2Cl_2 gave 65% **4**⊙8-hydroxy-8-methylbenzocyclobutene-7-one (**4⊙13**) and 25% **4**⊙9-methylphthalide (**4⊙14**). The following are the data for **4⊙13**. ^{1}H NMR (360 MHz, $CDCl_3$, 25 °C): δ 7.42 (d, 1H, guest-H), 7.16−7.25 (m, 40H), 6.87 (s, 8H,), 6.8 (t, 1H, guest-H), 5.71 (d, 8H), 4.93 (d, 1H, guest-H), 4.82 (t, 8H), 4.0−4.7 (m, 24H), 4.00 (d, 1H, guest-H), 2.86 (s, 1H, guest-O*H*), 2.47−2.75 (m, 32H), 1.87 (br s, 16H), −2.04 (s, 3H, guest-CH_3). FT-IR ($CHCl_3$, 25 °C, cm^{-1}): ν(CO) 1762. FAB-MS: *m*/*z* $[M + H]^+$, 2397 (84); $[M - \mathbf{13} + H]^+$, 2250 (100). Anal. Calcd for $C_{153}H_{144}O_{26}$: C, 76.61; H, 6.05. Found: C, 76.30; H, 6.17.

Methyllithium Addition to 4⊙3 at 0 °C. Application of procedure D to hemicarceplex **4⊙3** (0 °C, 8 h) and purification

of the reaction product by preparative TLC on SiO_2 with CH_2Cl_2 as the mobile phase gave 65% hemicarcerand **19** (X = H).

***n*-Butyllithium Addition to 4⊙3 at −78 °C.** Application of procedure D to hemicarceplex **4⊙3** (hexane/THF (1:5), 0.4 M *n*-BuLi, 0.2 M TMEDA, −78 °C, 12 h) and purification of the reaction product by preparative TLC on SiO_2 with CH_2Cl_2 as the mobile phase gave 10% hemicarcerand **19** (X = H), 10% hemicarcerand **20** (X = H), and 62% recovered **4⊙3**. The following are the data for **20** (X = H). ^{1}H NMR (400 MHz, $CDCl_3$, 25 °C): δ 7.15−7.30 (m, 40H), 6.89 (s, 1H), 6.896 (s, 2H), 6.85 (s, 1H), 6.84 (s, 2H), 6.81 (s, 2H), 6.59 (s, 1H), 6.06 (d, 1H), 5.97 (d, 2H), 5.87 (d, 2H), 5.86 (d, 2H), 5.82 (m, 1H) 5.07−5.21 (m, 2H), 4.85 (t, 2 H), 4.83 (t, 4H), 4.81 (t, 2H), 4.28 (m, 2 H), 4.27 (d, 2 H), 4.23 (d, 2 H), 4.20 (d, 2 H), 4.16 (dd, 2 H), 3.8−4.0 (m, 12 H), 2.10−2.75 (m, 34H), 2.1−1.75 (m, 14H). FAB-MS: *m*/*z* $[M + H]^+$, 2251 (100). Anal. Calcd for $C_{144}H_{138}O_{24}$: C, 76.85; H, 6.09. Found: C, 76.36; H, 6.01.

Methyllithium Addition to 4⊙2 at 22 °C. Application of procedure D to hemicarceplex **4⊙2** (22 °C, 5 h) gave 25% hemicarceplex **4⊙7**-methylbenzocyclobuten-7-ol (**4⊙22**), 1% hemicarceplex **4⊙23**, 40% hemicarceplex **24⊙23**, and 25% hemicarcerand **24** as determined from the ^{1}H NMR spectrum of the crude products. Purification of the reaction products was achieved by preparative TLC on SiO_2 with CH_2Cl_2 as the mobile phase. The following are the data for **4⊙22**. ^{1}H NMR (400 MHz, $CDCl_3$, 25 °C): δ 7.16−7.25 (m, 40H,), 6.94 (s, 8H), 5.93 (d, 1H, guest), 5.64 (d, 8H), 5.39 (d, 1H, guest), 4.98 (t, 1H, guest), 4.83 (t, 8H), 4.53−4.48 (m, 2H, guest), 4.33 (d, 8H), 3.97 (s, 16H), 4.00 (d, 1H, guest-H), 2.47−2.75 (m, 32H), 1.9−1.8 (m, 17H), 1.67 (s, 1H, guest), 0.90 (s, 3H, C*H*$_3$). FT-IR ($CHCl_3$, 25 °C, cm^{-1}): ν 3016 (m), 2947 (m), 2873 (w), 1603 (w), 1496 (w), 1474 (m), 1440 (s), 1374 (w), 1316 (m) 1224 (m), 1154 (m), 1106 (m) 1064 (m), 1018 (m) 988 (s). FAB-MS: *m*/*z* $[M + H]^+$, 2384 (38); $[M - \mathbf{19} + H]^+$, 2251 (100). Anal. Calcd for $C_{153}H_{148}O_{25}$: C, 76.99; H, 6.25. Found: C, 76.81; H, 5.98. The following are the data for **24**. ^{1}H NMR (360 MHz, $CDCl_3$, 25 °C): δ 7.72 (br s, 2H, OH), 7.10−7.30 (m, 40H, C_6H_5), 6.97 (s, 2H, Ar*H* on bowl), 6.88 (s, 2H, Ar*H* on bowl), 6.85 (s, 2H, Ar*H* on bowl), 6.84 (s, 2H, Ar*H* on bowl), 5.98 (d, 1H, OC*H*$_2$O outer), 5.92 (d, 3H, OC*H*$_2$O outer), 5.83 (d, 2H, OC*H*$_2$O outer), 5.71 (d, 1H, O OC*H*$_2$O outer), 4.75−4.9 (t, 7 H, C*H* methine), 4.61 (t, 1H, C*H* methine), 4.53 (m, 2 H, OC*H*$_2$CH$_2$), 4.34 (d, 2 H, OC*H*$_2$O inner), 4.14−4.28 (m, 7H, OC*H*$_2$O inner, OC*H*$_2$CH$_2$), 3.75−4.07 (m, 12H, OC*H*$_2$O inner OC*H*$_2$CH$_2$), 2.10−2.75 (m, 32H, C*H*$_2$C*H*$_2$Ph), 2.1−1.75 (m, 16H, OCH$_2$C*H*$_2$). FT-IR ($CHCl_3$, 25 °C, cm^{-1}): ν 3350 (v br) 3011 (m), 2948 (m), 2874 (m), 1602 (w), 1578 (w), 1496 (w) 1474 (s), 1441 (s), 1374 (m), 1317 (s), 1154 (m) 1106 (m), 1065 (m), 1018 (s), 988 (s). FAB-MS: *m*/*z* $[M + H]^+$, 2238 (100). Anal. Calcd for $C_{143}H_{136}O_{24}\cdot CH_2Cl_2$: C, 74.43; H, 5.99. Found: C, 74.57; H, 5.83.

Methyllithium Addition to 4⊙NMP at 0 °C. Application of procedure D to hemicarceplex **4**⊙NMP (THF/ether (1:1), 0 °C, 70 h) and purification of the reaction product by preparative TLC on SiO_2 with $CHCl_3$ as the mobile phase gave 70% hemicarcerand **24**.

X-ray Diffraction. Crystal data common to all three structures: **4**⊙guest·2$C_6H_5NO_2$ (crystallized from $CHCl_3$/$C_6H_5NO_2$, structure determined at 25 °C), $P2_1/c$, $\theta_{max} = 50°$, Cu Kα radiation. The host is centrosymmetric; the noncentrosymmetric guests are disordered about the center of symmetry in the host cavity. Two of the four bridges (linkers) that join the host bowls are also disordered. Each guest was modeled as a rigid group or groups. One molecule of nitrobenzene is located in each of the cavities formed by the four $-CH_2CH_2C_6H_5$ "feet". The present structures belong to an isomorphous series of nitrobenzene solvates of the same host with different guests.[19] The Crystallographic Information Files (CIF) are available as Supporting Information and have been deposited with the Cambridge Crystallographic Data Center (CCDC 196141, CCDC 196142, CCDC 196143).

Hemicarceplex **4⊙1**·2$C_6H_5NO_2$: a = 16.736(13) Å, b = 20.479(15) Å, c = 20.138(14) Å, β = 99.53(2)°, V = 6809(2) Å^3, Z = 2, 6870 unique reflections, 2461 > 2$\sigma(I)$, GOF = 1.730, R = 0.20 (295 parameters). The guest was refined as two independent rigid groups, nearly orthogonal to each other (89°) at convergence.

Hemicarceplex **4⊙2**·2$C_6H_5NO_2$: a = 16.650(11) Å, b = 20.442(14) Å, c = 20.043(13) Å, β = 98.998(16)°, V = 6738(8) Å^3, Z = 2, 6721 unique reflections, 2965 > 2$\sigma(I)$, GOF = 1.668, R = 0.17 (334 parameters). Internal coordinates for the guest, taken from the energy-minimized structure (Figure 12), are similar to those for benzocyclobutenone 1-oxime.[41]

Hemicarceplex **4⊙3**·2$C_6H_5NO_2$: a = 16.720(7) Å, b = 20.559-(8) Å, c = 20.168(8) Å, β = 98.524(12)°, V = 6856(5) Å^3, Z = 2, 6593 unique reflections, 2795 > 2$\sigma(I)$, GOF = 1.536, R = 0.16 (300 parameters). Approximate internal coordinates for the guest were taken from the structure of benzocyclobutenedione.[42]

Acknowledgment. We thank Professor Kendall N. Houk and Professor Harold W. Moore for helpful discussions and Dr. Rachel A. Watson-Clark for her assistance with recording the ^{11}B NMR spectrum. We thank the U.S. Public Health Service for supporting Grant GM-12640 (D.J.C., principal investigator). The major part of this work was conducted at UCLA. R.W. thanks the Alexander von Humboldt Foundation (Germany) for a Feodor-Lynen fellowship and Kansas State University for startup funds to continue this work at Kansas State University.

Supporting Information Available: ^{11}B NMR spectrum of **4⊙9**, COSY spectrum of **4⊙7**, **4⊙9**, **4⊙10**, **24⊙23**, and **24**, TOCSY spectrum of **24⊙14**, H/D exchange experiments of **24⊙23**, and Crystallographic Information File (CIF) for **4⊙1**, **4⊙2**, and **4⊙3**. This material is available free of charge via the Internet at http://pubs.acs.org.

JO026649Z

(41) Viossat, B.; Rodier, N.; Andrieux, J.; Plat, M. *Acta Crystallogr.* **1986**, *C42*, 824−825.
(42) Allen, F. H.; Trotter, J. *J. Chem. Soc. B* **1970**, 916−920.